Effects of geological characteristics on the kinematics of Hungtsaiping landslide during earthquake events

Wei-Kai Huang* · Chia-Ming Lo · Ming-Lang Lin · Jia-Jyun Dong · Kuang-Tsung Chang · Shu- Yung Chi

Abstract. The Chi-chi earthquake triggered a large, 100 hectare, deep-seated landslide in the Huangtsaiping area of Nantou county in 1999. Through field investigations, an irregular pattern of displacement vectors was identified, making this failure very complex. Landslide site investigations included field reconnaissance, geomorphologic analysis, geophysical exploration, borehole logs, and laboratory experiments. The Hungtsaiping area involved at least three large landslide events, two ancient rockslides (the first triggered during the 1916 Nantou earthquake and other event occurring after 1934) and the 1999 colluvium slide (triggered during the 1999 Chi-chi earthquake). With the consideration of a source collapse mass, three landslide events were reasonably reproduced using a 3D discrete element model. The numerical model parameters were calibrated using rock mass strength behavior and the morphology of the landslide deposits.

Keywords:Earthquake, Landslide, 3D discrete element modeling

Introduction

The Nantou earthquakes were a series of earthquakes which affected central Taiwan in 1916 and 1917, causing heavy damage in sparsely populated Nantou County and claiming 71 lives. The strongest quake registered at 6.8 ML and besides the loss of life caused widespread damage to agricultural and forestry industries in central Taiwan(Cheng and Yeh,2001). The Chi-Chi earthquake, which occurred on September 21, 1999 with the Richter magnitude of 7.3 and its epicenter at Chi-Chi city, triggered more than 9000 landslides over 128 km^2 in the central mountain area of the island (Liao, 2000). Nantou county was the most seriously affected, where several fast and catastrophic landslides occurred, such as the Jiufengershan and Tsaoling landslide. On the other hand, a slow deep-seated landslide induced by the earthquake was noticed at Hungtsaiping in Nantou county (Lee et al., 2004; Wei and Lee, 2006). Deep-seated mass movements are not well understood due to their large scale of deformation, limited applicability and the cost of ground surveys. However, several large gravitational failures cases have been described that highlight the landslide kinematics is important (e.g. Chang et al., 2005; Dong et al., 2009; Lo et al., 2011). Moreover, large, high velocity landslide, especially the disintegrative rockslide that develop into debris avalanches (sturzstroms) are remarkable geological phenomena (Steven and Simon, 2006). A deep-seated landslides in Huntsaiping are commonly covered by colluvium that was caused by ancient landslides (Chang et al., 2008; Lo et al.,2008). The mechanism of Huntsaiping landslide was complex that caused the kinematics and geomorphology development were very difficult to interpret for each events.

Dong (2009) concluded that the seismic anisotropy, sliding direction, and mechanical properties of sliding surface are important contributing factors to the kinematics of landslide. However, a complex kinematics of Hungtsaiping landslide need appropriate numerical analysis to simulate movement process for each events that will understand the landslide mechanism and kinematics will helpful for mitigation strategies, or predict possible future landform processes.

In view of this, that in order to simulate the sliding material, through field investigation noticed the landslides often involve heterogeneous granular materials such as rocks and debris, the discrete element method is appropriate for the analysis of the sliding process, and also the authoritative tool to simulate the kinematics of landslide movement (e.g. Chang et al., 2005; Tang et al., 2009; Lo et al.,2011). Chang (2011) used 2D discrete element model concluded the model can reasonably reproduce the ancient rock slide and the 1999 colluvium slide at Hungtsaiping, but the runout of the ancient rockslide only considered in a straight path due to the 2D topographic effects, that neglected the diffusion characteristic for 3D complex terrain in Hungtsaiping.

Summary the above conclusions, the complex slope collapse mechanism of the sliding mass depends on the morphological and geological characteristics, the rheology of sliding materials, and the triggering condition. Thus, the study described the geological characteristics in the Hungtsaiping during the Nantou earthquake (1916) and Chi-chi earthquake (1999) events using a 3D discrete element model based on the theory of granular mechanical that aim to:

(a) simuler movement process of the Hungtsaiping landslide for each events during earthquake events.
(b) establish the relationship between the geological characteristics and the landslide kinematics.

Terrain of the Hungtsaiping Landslide

The evidence of the geomorphic features that provided the activity of past landslides and potential unstable zones. Furthermore, topographic maps show the size, shape, and depiction of the landslide area. The orthographic topographic maps, at scales of 1:20000, 1:25000 and 1:50000 released in 1904, 1934, 1998, 2003 respectively, were used interpreted geomorphic features of landslide (Fig.1). The Yonglu stream played a crucial role in the study area. The Nantou series of earthquake events (1916-1917) caused the first landslide between 1904 to 1934.The sliding mass deflected the Yonglu stream toward northwest. This event caused the toe of sliding mass III daylight and instability, that provided condition of the dip slope failure after 1934. Chi-chi earthquake caused sliding mass I and III slip displacements of about 28 meters between in 1999 (Lee et al., 2004).

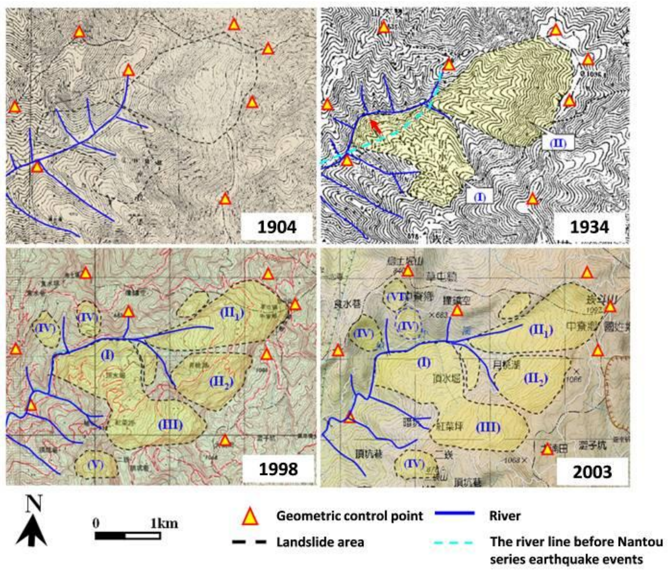

Fig 1. Topographic maps showing the location of the Hungtsaiping landslide

The relationship of past seismicity and Nantou & Chi-Chi earthquake of the Hungtsaiping

Taiwan is located in an active curved collision belt which developed as the result of the late Cenozoic oblique collision between the Philippine and the Eurasian plate (Suppe, 1984; Barrier, 1986; Angelier etal,. 1990; Teng, 1990 Huang et al., 1992; Lu and Hsu, 1992). This extension system has developed the Pei-Kang basement High (PKH)(Fig.2 a) in the middle of western Taiwan, which latter acts as a barrier to block the Pilippine Sea Plate's (PSP) movement, cause a large amount of seismicity in the Chianan area of the western Taiwan (Wang et al., 1998).

Wang(2000) concludes in the past 100 years, the seismic activity in western central Taiwan can be grouped into two different zones. The one in the north, the seismicity forms a linear pattern trending in the NW-SE direction, called the Tunghsiao-Puli Linear seismic zone (TPL). The seismic zone south of the Choshuihsi stream near Chia-Yi, called the Chia-Yi Group seismic zone (CYG). Before the Chi-Chi earthquake, we did not realize why there were two separated seismic zones in central Taiwan. Thus, we began to understand that could actually be only one seismic zone, rather than two, surrounding the PKH. All these fact clearly indicate that the TPL seismic zone is linked with the CYG seismic zone to from semi-circular belt surrounding the PHK(Fig.2 b).

The seismicity were distributed in this semi-circular belt rather than associated with the Chelungpu fault which had been activated by the main shock. More interestingly, the earthquake focal mechanisms for some of these big aftershock were almost the same as that of the main shock (Wang et al., 2000). Therefore, the similar geological structure occurred the Nantou earthquake, based on this statement, we used the same location, depth, and magnitude to simulate the PGA waveform that in the Chi-Chi earthquake aftershock, attempt to simulate the vibrations force of Nantou earthquake, and actual measurement strong motion data to simulate the vibrations force of Chi-Chi earthquake, that triggered the deep-seated landslides in Huntsaiping.

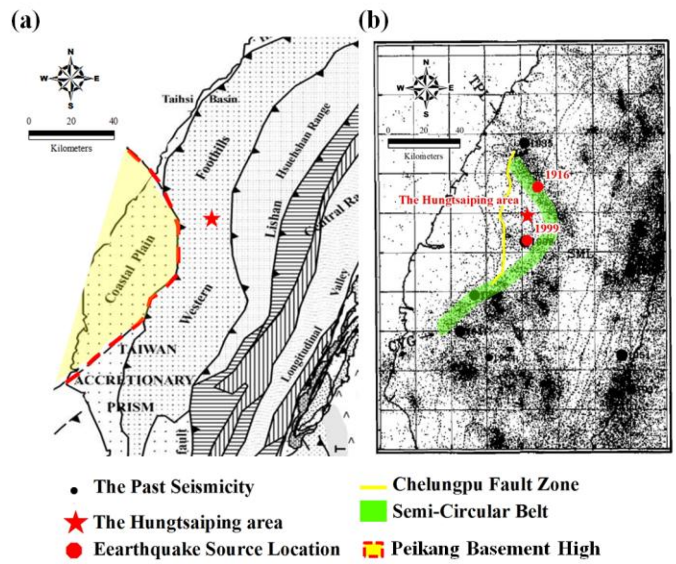

Fig 2. The tectonic and past seismicity source location of Taiwan western area.

a. The tectonic boundary of Peikang Basement High (modified by Huang et al., 2001).
b. The relationship of semi-circular belt and 1916,1999 earthquake source location(modified by Wang et al., 2000).

Geology investigation and borehole logs of the Hungtsaiping

The geological map of Hungtsaiping area is the main reference for simulate model based on geology investigation shown in Fig.3. The axis of the Syncline was constrained by the measured orientation of the bedding planes. M-symmetry minor folds of thin-bedded siltstone and sandstone layers within a massive shale (Tanliaoti Shale) crop out on the river bank of Yonglu stream (Fig.3 a), and these M folds should coincide with the hinge of a large fold structure (Dong et al., 2009).

According to results of borehole logs and RIP (resistivity image profiling) (Fig.3b). The interface between the shale and the colluvium was mainly a bedding plane. Before the 1999 colluvium slide, an ancient rockslide was speculated to cause the thick colluvium. The possible source is the massive sandstone exposed at the southeast of the slide area, where the current sandstone appears as scarps and steep slopes. The ancient rock mass composed mainly of sandstone might have slide along a surface that was in the underlying shale under certain unstable conditions, such as those caused by raining or earthquake(Chang et al., 2011).

Comprehensive results of the geology investigation and borehole logs survey and mapping of the underlain strata of Hungtsaiping landslide are shown in Fig.3c. The numerical modeling was reconstructed the past landslide process duringearthquake events base on the geological map, which helpful for explain effect of geological characteristics on the kinematics of Hungtsaiping landslide.

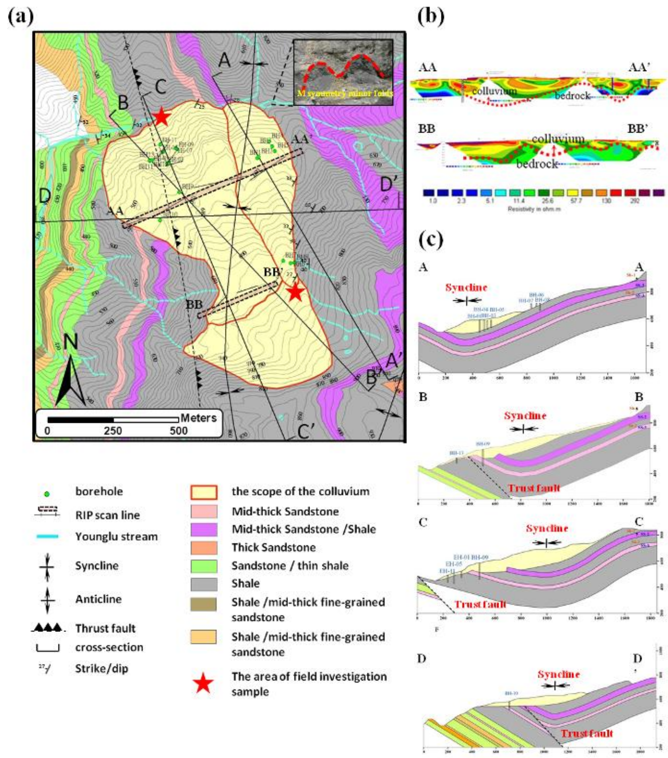

Fig 3. The geology investigation and borehole logs surveying and mapping the underlain strata of Hungtsaiping landslide, and locations of boreholes and resistivity exploration.

a. The geological map of the landslide area.
b. Profile AA-AA' and BB-BB' across the slide directions with resistivity survey lines(Chang et al., 2011).
c. Cross-sections A-A', B-B', C-C', and D-D' show the topography, geological structures and underlain strata (Dong et al., 2009).

Numerical Simulation Concept

The numerical PFC (Particle Flow Code), models sphere particle movement, interaction, and the particle velocity and up-to-date position using the Discrete Element Method (Cundall and Strack, 1979), based on the theory of Newton's 2nd law. In the course of the calculation the contacts between particles and particles or particles and walls are detected automatically. The particles may be bonded together at their contact points, and the bondage can break due to an impact. In general, the fundamental assumptions for PFC model are indicated as follows: (a) each element is a perfect sphere and considered as a rigid body. By means of the combination command of "Clump", the particles can be formed in various shapes composed of different amount of elements; (b) PFC allows the overlap of adjacent particles. The overlap extent is related to the contact force and stiffness of particles based on the force-displacement relations; (c) strength is exhibited between two particles through the contact bond or the parallel bond. The parallel bond is composed of a set of virtual springs which have effect in vertical and tangential directions, transferring not only stress, but also moment. The contact bond can only transfer force; these bonds can fracture gradually when the mass is under stress or moving, and separate into mutually independent mass, the displacement distance is free from any limit within the allowable range of program (Tang et al, 2009).

Above-mentioned of dynamic behavior was represented numerically by a time stepping algorithm in which it was assumed that the velocities and accelerations were constant within each time step. The use of an explicit, as opposed to an implicit, numerical scheme makes it possible to simulate the nonlinear interaction of a large number of particles without excessive memory requirements or the need for an iterative procedure (Itasca, 2002). Therefore, in the whole simulation model the time step played a critical parameter, that might be affect performance and efficacy of system calculation. The study compared different time steps of Hungtsaiping landslide simulation, the major comparison basis included the length and the width of landslide zonation, and then 0.005(sec/step) was chosen to set time step parameter (Fig.5).

3D numerical model of the Hungtsaiping landslide

The Discrete Element Method does not limit the scale of separation and displacement behaviors of elements, and the movement process of the mass from fracture to separation can be fully simulated, so it is very applicable to the simulation of landslides (Poisel and Roth, 2004; Poisel et al., 2005). Hence this paper used PFC 3D to simulate and interpret the kinematic process of the Hungtsaiping landslide of three events. The elements of PFC model mainly include particles and walls, the sliding surface of the collapse area in the Hungtsaiping landslide model was constructed by 87,000 wall elements based on a 15×15m DEM from the mapping of underlain strata and geologic structure. An attempt to reconstruct the geological structure sliding surface before the 1904 Nantou series earthquake events is shown in Fig.4a. The total length from east to west was 3,765m, the total width from south to north was 2,625m. The sliding mass of the Hungtsaiping landslide was constructed using 20,158 spherical elements with a radius of 7.5 meters and the 18,379 spherical elements were divided into three blocks (Fig.4b, 5a); the total volume was about 33 million cubic meters.

The macroscopic behaviour of the granular media depends on the contact mechanical properties, but there is no straightforward solution relating these parameters. To use PFC models as reliable simulation tools, it is necessary to establish reasonable relations between the numerical parameters and the mechanical characteristics of real problems (Potyondy and Cundall, 2004). Recently, application of experimental design and optimization to PFC model calibration in uniaxial compression test was proposed to calculate proper macro-parameters for model generation in order to closely reproduce macro-parameters of the rock material such as uniaxial compression strength (UCS), Young's modulus and Poisson's ratio (Yoon, 2007). For bond model, the macro-parameters for interaction of two circular particles are normal and shear stiffness, normal and shear bonds, and Coulomb friction coefficient must be obtained during the calibration step. Fakhimi (2004) proposed a slightly overlapped circular particle interaction to resolve the failure envelope and the ratio of unconfined compressive strength to tensile strength which is usually lower than that of a rock. An application of dimensional analysis in calibration of a discrete element method for Sandstone was carried out to mimic the deformational and failure characteristics in stress paths (Fakhimi and Villegas, 2007). Although there is no straightforward solution from micro-properties to macro-parameters, some relations exist between the two properties for initial calibration as follows. The Young's modules of the grains and cement are expressed by:

$$E_c = \frac{k_n}{4R} \qquad [1]$$

Where kn and R are particle normal stiffness and particle radius (Potyondy and Cundall, 2004). Thus, Poisson's ratio depends both on the ratio of shear contact stiffness to normal contact stiffness and packing geometry. The peak strength of the material depends both on the friction coefficient and the bond strength (Itasca, 2002).

Thus we performed a series of compression numerical tests on granular samples to derive the rock mechanical macro-properties, and take field investigation sample (Fig.6a., b.) to modify strength properties of Hungtsaiping sandstone borehole logs result (Chang et al., 2011) by the Hoek – Brown failure criterion (Fig.6c., d.). The 3D granular sample consists of 8574 spherical elements. The numerical parameters obtained for a compression test are the Young's modulus E=407.21MPa, and the compression strength UCS=5.249MPa. The internal friction angle is 17.63° (Fig.6e). The macroscopic properties of the numerical sample are similar to the properties of the rock samples from the sandstone, as determined from laboratory tests (Tab.1). Tab.2 is the numerical parameters used for PFC modeling.

The numerical model of Hungtsaiping landslide were reconstructed into three landslide events that explain as follow:

1. First landslide event: The Nantou series of earthquake events caused the first landslide between 1904 to 1934, which possiblly caused the massive sandstone exposed at the southeast of the slide area, where the current sandstone appears as scarps and steep slopes (mass A, mass B, and mass C). According to the simulation result, this triggered during the 1904 to 1934 Nantou series earthquake. In this case that gave the gravity to simulated landslide after earthquake events while the rock mass C movement, the mass B slide almost entirely collapsed, cause the thick colluviums that deflected the Yonglu stream toward northwest (Fig.5b).
2. Second landslide event: After the Nantou series of earthquake events caused the first landslide. The mass B and mass C trigged by ground motion, caused mass A to loose support, and collapse under the influence of gravity (Fig.5c, d).
3. Chi-chi earthquake event: The ancient landslide model which results in deposition at the down slope, proceeds for the simulation of the 1999 landslide. The deposit in the creek valley is eliminated as the geological process of erosion before the earthquake. The strong motion records collected at the station TCU072 (Fig.7), which is 10 km away, is used for earthquake loading (Fig.5e). Using the ball elements of sliding mass to record sliding displacement, the maximum displacement is 25.6 m, and the displacement of elements are shown in Fig.8.

Table 1. The comparison results of uniaxial compression test by the Hoek–Brown failure criterion and PFC Model.

Item	sandstone mass estimated by the Hoek–Brown failure criterion	PFC Model (Marco-properties)
Density	2,600 kg/m^3	2,600 kg/m^3
Young's Modulus (Ec)	407.21MPa	407.23MPa
UCS	5.249MPa	5.251MPa

Table 2 The numerical parameters of PFC modeling.

	The numerical parameters of compression test	The numerical parameters of the landslide
Number of wall elements	2	87,000
Number of particles	2,650	18,379
Particle density (kg/m^3)	2,600	2,600
Range of particle radius (m)	0.075-0.1	7.5
Normal stiffness (KN/m)	1.42e8	1.22e10
Shear stiffness (KN/m)	0.56e8	0.61e10
Friction coefficient of ball	0.5	0.3
Friction coefficient of wall	0.5	0.3
Normal stiffness of parallel bonds (KN/m^3)	2.39e9	2.71e7

Shear stiffness of parallel bonds (KN/m^3)	1.19e9	1.35e7
Normal strength of parallel bonds (Mpa)	5.2	5.2
Shear strength of parallel bonds (MPa)	2.6	2.6

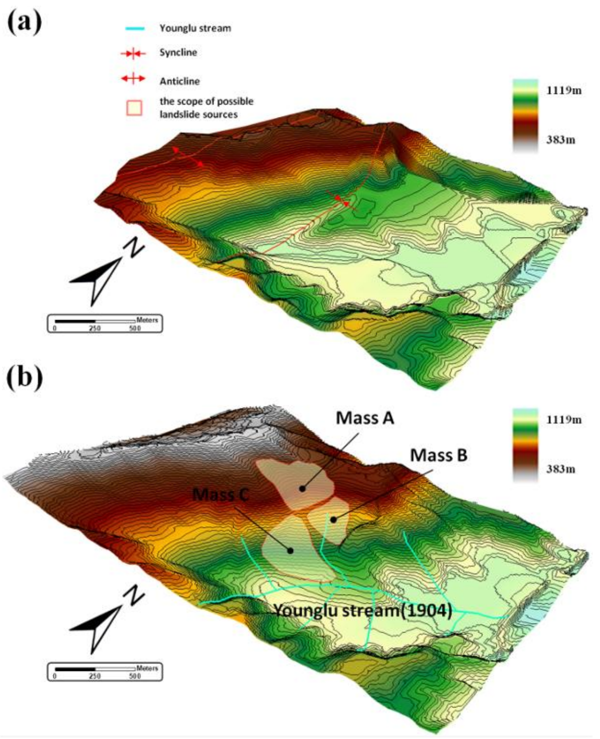

Fig 4. A 3D geological layer, base on the mapping of underlain strata

a. A 3D geological layer of mid-thick sandstone, and include geological structure of syncline and anticline.

b. A 3D geological layer of shale, that reconstructed sliding surface base on **Fig 4. a.**, and modifed by topographic maps from 1904. And the scope of possible landslide sources: mass A, mass B, massC.

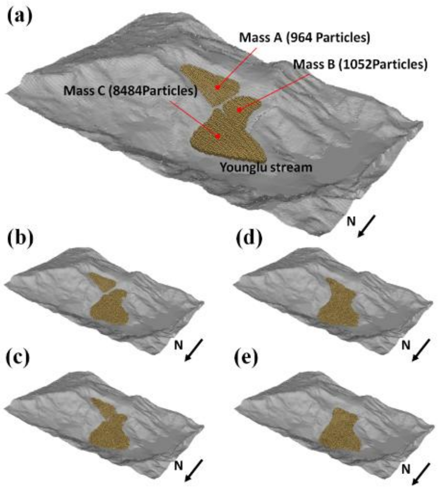

Fig 5. The numerical modeling of the Hungtsaiping landslide.

a. The Hungtsaiping landslide model was constructed using wall and ball elements constructed**.**

b. Simulations of the first landslide event during the Nantou series of earthquake events.

c., d. Simulation of after the Nantou series of earthquake events caused the second landslide event. The mass A lost support, and collapsed under the influence of gravity.

e. Simulation of after the Chi-chi earthquake events caused the ancient landslide movement.

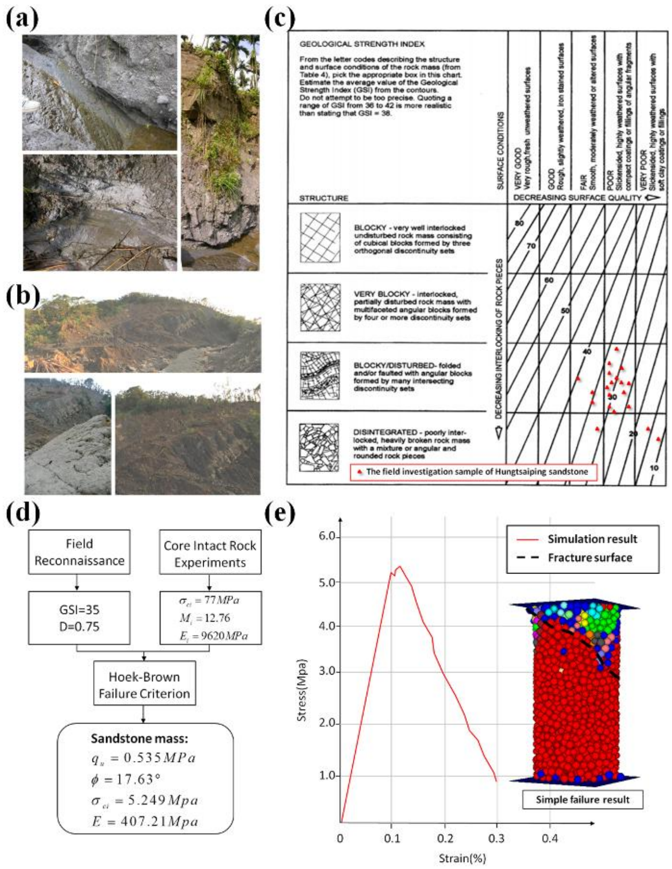

Fig 6. The field investigation sample to modify strength properties of Hungtsaiping sandstone borehole logs result (Chang et al., 2011) by the Hoek – Brown failure criterion and simulation uniaxial compression test..

a. The field investigation area of Fig 3a., the middle of slope.

b. The field investigation area of Fig 3a., the slope toe .

c. The geological strength index and field investigation sample distribution.

d. The intact rock parameter (Mi) determined by fitting the data of Brazilian, uniaxial compression, and triaxial compression tests b Strength properties of sandstone mass estimated by the Hoek – Brown failure criterion

e. The comparison result of simulation uniaxial compression test.

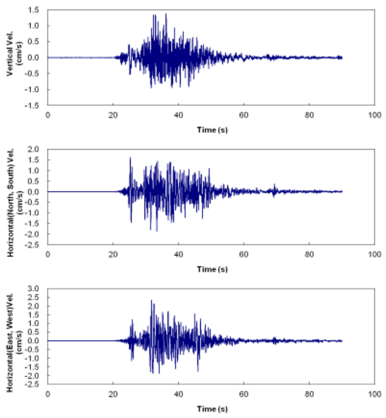

Fig 7. Seismic records at TCU072 in the vertical, North-South, and Eeast-West directions.

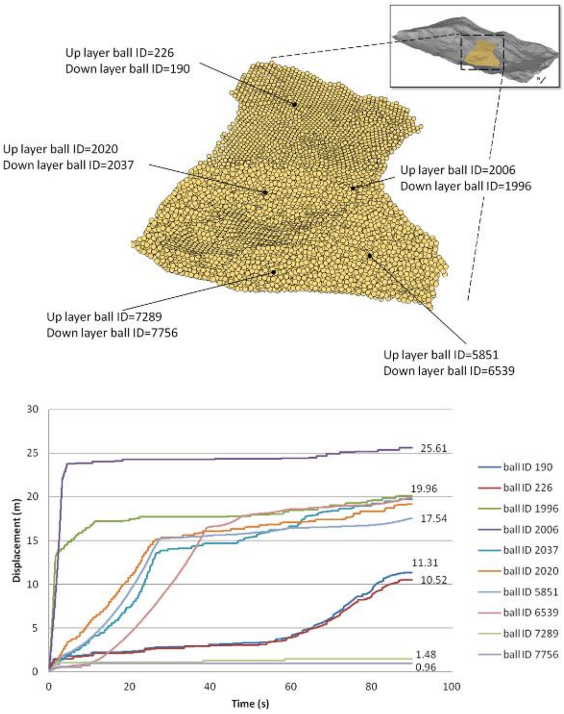

Fig 8. The sliding mass location, and displacement of ball elements.

Discussion and conclusions

Our Discrete Element numerical modeling of the three event-caused landslide brings important physical constraints that can be compared with, and controlled by, field observations and reported disaster characteristics of those events. The research of the Nantou series earthquake, Chi-Chi earthquake (Lo et al.,2008; Chang et al.,2011; Lee et al., 1999) and earlier studies associated with those earthquakes provided abundant background information to explore the possible factors that govern the kinematics of the large earthquake-induced landslides. Based on previous studies to build numerical simulation, we can discuss in more details the possible reasons for slide mass movement after the events. After the simulation results by PFC3D compared with the particle image velocimetry technology (PIV) (Lo et al.,2008) in Chi-Chi earthquake event, the boundary and movement direction of colluvium were almost matched (Fig.9), and therefore had same conditions worth exploring. In the field, we found evidence of a Syncline, that is M-symmetry minor folds of thin-bedded siltstone and sandstone layers within a massive shale (Tanliaoti Shale) crop out on the river bank of Yonglu stream, which played aa crucial role for this study area. It controlled sliding direction, let the sliding mass (Fig.5b mass B, mass C) after Nantou series earthquakes turned northwest to north and deflected the Yonglu stream toward northwest between 1904 to 1934. This event caused the toe of sliding mass A to daylight and and become unstabile, which provided conditions for the dip slope failure after 1934. Chi-chi earthquake caused sliding mass A, B, and C slip displacement of about 25.61 meters between 1998 to 2003. Conditions of this case are worth discussing.

After in the simulation, the area of ball ID 2020 and 2037 around had large displacement of about 19.1 m. On the other hand, the area of ball ID 7289 and 7756 around at the lower slope that only had displacement about 1.48 m. The conditions of such a large differences in displacement may have caused deformation of the mass of colluvium and resulted in tension cracks developing on the sliding surface.

The discrete element method is suitable for the modeling of landslides with long runout provided that the determination of the micro-parameters can be reasonably solved for according to the mechanical behavior of the geomaterials on slopes.

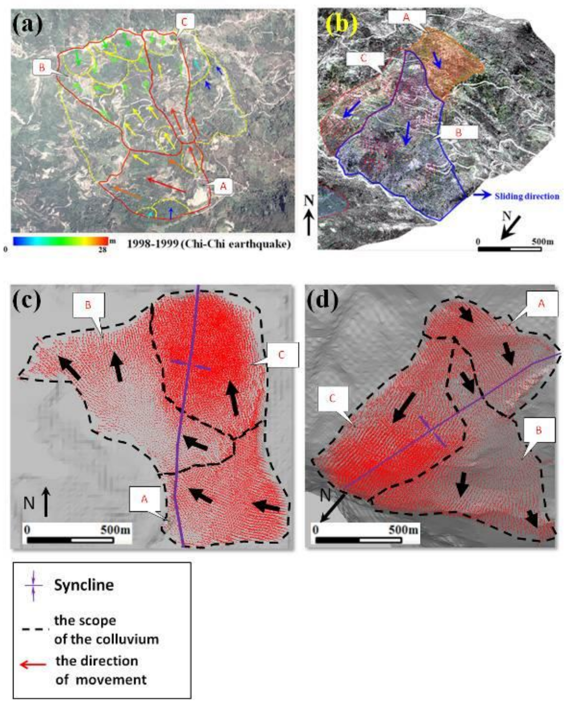

Fig 9. The results of simulation during Chi-chi earthquake events.

a., b. The surface displacement identified morphologic changes by the particle image velocimetry technology (PIV) for detailed landslide zonation with topographic maps (Lo et al., 2008).

c., d. The surface displacements identified by PFC 3D for simulated kinematics of Hungtsaiping landslide.

References

Chang KJ, Taboada A, Chan YC (2005) Geological and morphological study of the Jiufengershan landslide triggered by the Chi-Chi Taiwan earthquake. Geomorphology 71(3-4):293-309.

Chang KT, Lai CC, Lin DG (2008) Analyses of the Huntsaiping Landslide Induced by the Chichi Earthquake, Journal of Chinese Soil and Water Conservation, 39(3): 329-344 (in Chinese).

Chang KT, Lin ML, Dong JJ, Chien CH (2011) The Hungtsaiping landslides: from ancient to recent, Landslides (3 September 2011), 1-10

Cundall P A (1971) A computer model for simulating progressive large scale movement in blocky rock systems. Proceedings of the Symposium of the International society of rock mechanics, 1. Nancy, France, II-8.

Cundall P A, Strack OD (1979) A discrete numerical model for granular assemblies. Geotechnique 29: 47-65.

Dong JJ, Lee WR, Lin ML, Huang AB, Lee YL (2009) Effects of seismic anisotropy and geological characteristics on the kinematics of the neighboring Jiufengershan and Hungtsaiping landslides during Chi-Chi earthquake. Tectonophysics 466(3–4):438–457

Fakhimi A, Villegas T (2007) Application of dmensional anlysis in calibration of a discrete element model for rock deformation and fracture. Rock Mechanics and Rock Engineering 40: 193-211.

Itasca, Consulting Group Inc (2002) PFC3D Particle Flow Code in 3 Dimensions. User's Guide. Minneapolis.

Lee JF, Wei CY, Huang CC (2004) The study of Hungtsaiping landslide using digital photogrametric technique. Proceeding of International Symposium on Landslide and Debris Flow Hazard Assessment, 2004 Oct 7th–8th, Taiwan, pp. 5–1–5-9.

Lee WHK, Shin TC, Kuo KW, Chen KC, Wu CF (1999) CWB free field strong-motion data from the 921 Chi-Chi earthquake: volume 1. Digital Acceleration Files on CD-ROM.

Liao HW (2000) Landslides triggered by Chi-Chi earthquake. Master's thesis, Institute of Geophysics, National Central University (in Chinese).

Lo CM, Lin ML, Lee WC, Lee KC, Chien SY, Dong JJ, Chang KT, Huang AB (2008) Landslide characterization and zonation of Hungtsaiping area based on topography, aerial photograph and PIV technology. The 3rd International Conference on Site Characterization, Taipei, Taiwan, 1–4 April 2008, pp 467–472 (CD ROM)

Lo CM, Lin ML, Tang CL, Hu JC (2011) Kinematic Process of the Xiaolin Catastrophic Landslide, Eng Geol

Hoek, E., Carranza-Torres, C. and Corkum, B. (2002), Hoek-Brown Failure Criterion-2002 Edition, 5th North American Rock Mechanics Symposium and 17th Tunneling Association of Canada Conference: NARMS-TAC, pp. 267-271.

Poisel R, Roth W (2004) Runout models of rock slope failures. Felsbau 22: 46-50. Poisel R, Bednarik M, Holzer R, LIŠČÁK P (2005) Geomrchanics of Hazardous landslides. Journal of Mountain Science 2(3): 211-217.

Potyondy D, Cundall P (2004) A bonded-particle model for rock. International Journal of Rock Mechanics & Mining Sciences 41:1329–1364

Steven N W, Simon D (2006) Particulate kinematic simulations of debris avalanches: interpretation of deposits and landslide seismic signals of Mount Saint Helens, 1980 May 18. International Journal of geophysics 167: 991-1004.

Tang CL, Hu JC, Lin ML, Angelier J, Lu CY, Chan YC, Chu HT (2009) The Tsaoling landslide triggered by the Chi-Chi earthquake, Taiwan: insights from a discrete element simulation. Eng Geol 106:1–19

Wei CY, Lee JF (2006) The application of digital aerial photography in the study of Hungtsaiping landslide, Chungliao, Nantou County. Bulletin of the Central Geological Survey 19: 39–59 (in Chinese).

Yoon J (2007) Application of experimental design and optimization to PFC model calibration in uniaxial compression simulation. International Journal of Rock Mechanics & Mining Sciences 44:871–889